ELSEVIER

Ultramicroscopy 91 (2002) 133–138

ultramicroscopy

www.elsevier.com/locate/ultramic

An atomic force microscope-based investigation of vertical transport through GaAs/GaAlAs/InAlAs/GaAs step-barrier heterostructures

G. Muralidharan[a,*], D.M. Nicholson[a], S. Rajic[a], T.M. Daniels-Race[c], H. Li[c], T. Thundat[a,b], P.G. Datskos[a,b]

[a] *Oak Ridge National Laboratory, Oak Ridge, TN 37831, USA*
[b] *University of Tennessee, Knoxville, TN 37996, USA*
[c] *Duke University, Durham, NC 27708-0291, USA*

Received 27 June 2001; received in revised form 6 September 2001

Abstract

Study of vertical transport through heterostructures consisting of single, double, or multiple quantum barriers is of both fundamental and technological interest. While extensive data regarding electron transport is available for single- and double-barrier structures, relatively less information is available for transport through step-barrier structures. In this paper, we present results from a study of room temperature vertical transport through a GaAs/GaAlAs/InAlAs/GaAs multistep-barrier heterostructure. A typical atomic force microscope has been adapted to perform transport measurements, thus allowing precise control of the physical location of the region of measurement. $I-V$ measurements reveal negative differential resistance (NDR) peaks, thus confirming the formation of resonant states in a triangular well created when a voltage bias is applied across the step barrier. $I-V$ curves have also been calculated by numerically solving the Schrödinger wave equation for this step-barrier structure. Comparison between the measured and calculated $I-V$ curves shows reasonable agreement in the number of NDR peaks. However, discrepancies exist between the measured and calculated values for the voltages at which these NDR peaks occur. Some possible reasons for these discrepancies are discussed in this work. © 2002 Elsevier Science B.V. All rights reserved.

1. Introduction

Single- and double-barrier heterostructures have attracted considerable attention, in terms of both experimental and theoretical studies. Resonant tunneling and negative differential resistance (NDR) have been observed in these structures [1–5]. For example, in double-barrier heterostructures, it has been shown that bound resonant states develop in the well region sandwiched between the two barriers, resulting in NDR peaks [1,2]. While much work has been focussed on III–V compounds such as lattice-matched GaAs/AlGaAs and pseudomorphic InGaAs/AlGaAs [1–5], there has also been some work on Ge/Ge_xSe_{1-x} heterostructures [6]. Devices such as quantum well oscillators, memory devices, and switches have been proposed as potential applications for these heterostructures [2–5].

Recently, there has been some interest in the study of step-barrier heterostructures. Numerical

*Corresponding author.
E-mail address: g5m@ornl.gov (G. Muralidharan).

0304-3991/02/$ - see front matter © 2002 Elsevier Science B.V. All rights reserved.
PII: S0304-3991(02)00092-X

calculations and experimental work have shown that, similar to double barriers, NDR can be observed in step barriers [7–11]. Early work with $GaAs/Al_{0.2}Ga_{0.8}As/Al_{0.4}Ga_{0.6}As/GaAs$ step-barrier heterostructure showed evidence for NDR at 12 K [7]. More recently, experimental and theoretical work was conducted with a step barrier consisting of AlAs/GaAs layers [8,9]. Experiments showed evidence of an NDR peak around a voltage of 1.6 V–77 K and at 300 K [8]. However, calculations predicted the occurrence of an NDR peak at around 0.45 V. The authors ascribed this discrepancy to the poor quality of the layers and the device, and potential drop at contacts. In addition, the peak-to-valley current ratios (PVR) in these devices were very small [8]. It has been recently proposed that step barriers have outstanding properties for high-frequency and fast-switching applications and that larger PVR can be obtained by properly adjusting the parameters of step-barrier structures [10,11].

In this paper, we present preliminary results of a study on the vertical transport characteristics of a step-barrier heterostructure consisting of GaAs/GaAlAs/InAlAs/GaAs layers as shown in Fig. 1. This work is part of a comprehensive study on the effect of barrier heights and layer thicknesses on the PVRs in NDR observed at room temperature in step barriers. In contrast to traditional measurements that rely on the fabrication of structures with a lateral size of many tens of microns, in the present study, $I-V$ measurements have been carried out with a microcantilever tip coated with a metal layer on the underside acting as one of the electrodes. Contact diameter is estimated to be of the order of tens of nanometers. Although data obtained from micron-scaled structures would be more appropriate for characterizing typical device behavior, such data would be significantly influenced by the quality of the various layers and the interfaces over a relatively large area (many hundreds of square microns). It is expected that the data obtained with the use of the microcantilever would be less influenced by any nonuniformity of the heterostructures over this scale since the contact area is relatively small.

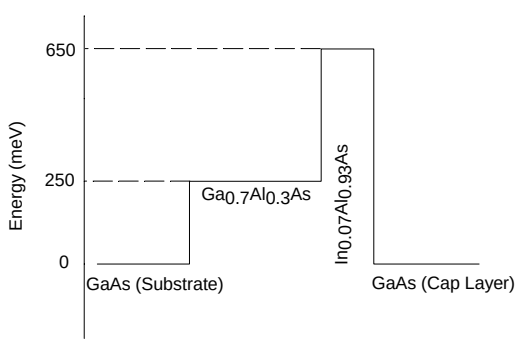

Fig. 1. Schematic showing the presence of the stepped barrier in the layered heterostructure.

2. Experimental procedure

A multilayered heterostructure consisting of a $Ga_{0.7}Al_{0.3}As$ layer, an $In_{0.07}Al_{0.93}As$ layer, and a cap layer of GaAs was grown on a GaAs substrate using molecular beam epitaxy (MBE). Samples were grown in a Riber 32 R&D MBE machine. Typical growth rates were 1 μm/h. In-situ characterization using reflection high energy electron diffraction was performed during pre-growth to ensure good morphology while not disturbing actual device layers. Growth temperatures were 600°C for the layers not containing indium, while the growth temperature was lowered to 540°C for layers containing indium to prevent excessive indium desorption during growth. Iterative growths on similar structures were made to check the control over layer thickness. The details of the composition and the thickness of the layers in the heterostructure are shown in Table 1.

$I-V$ measurements were carried out at room temperature and pressure using a setup based on an atomic force microscope. Fig. 2 shows a schematic of the setup. A multimode AFM base

Table 1
Composition of the multilayer step-barrier heterostructure

Material	Thickness (nm)	Function
GaAs	5×10^5	Substrate
$Ga_{0.7}Al_{0.3}As$	10	Barrier layer
$In_{0.07}Al_{0.93}As$	3	Barrier layer
GaAs	10	Capping layer

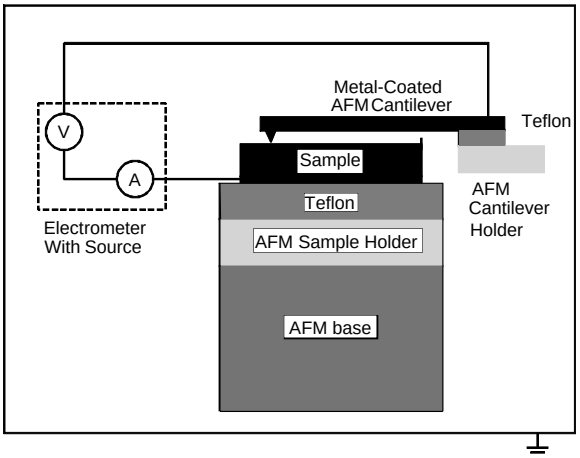

Fig. 2. AFM-based experimental setup for measuring vertical transport through the heterostructures.

was used along with its associated head. The sample was placed on top of a specially fabricated stack consisting of two metal plates separated by a layer of Teflon. The Teflon layer in the stack was used to isolate the sample from ground. The bottom plate of the stack was used to attach the sample to the magnetic base of the AFM, while the top plate is used to contact to the bottom of the sample. The top plate was used as one of the electrodes. A Si-cantilever with a layer of Au deposited on the bottom-side was used as the second electrode. The cantilever holder was also isolated from ground with a layer of Teflon. The complete experimental apparatus was placed in a shielded Faraday cage to minimize electrical interference. A Keithley 6517A sourcemeter (with a leakage current of a few fA) was used to apply the voltage and measure the current as a function of the voltage. Voltage was applied in steps of 5 mV.

3. Numerical calculations

In order to visualize $I-V$ curves that could result from step barriers, they were modeled as infinite and homogeneous in two dimensions with a step-wise continuous potential in the third direction. Potential values of 250 and 650 meV were assigned to the $Ga_{0.7}Al_{0.3}As$, and $In_{0.07}Al_{0.93}As$ layers, respectively, as shown in Fig. 1. The effective mass approximation was used with a mass of $0.067m_e$ for all layers. Defects that could reduce the electron mean free path were ignored, although it was estimated that for good samples, the electron coherence length at room temperature would be sufficiently long to allow interference effects from scattering at the material interfaces. It was anticipated that the sharpness of calculated features would depend on the quality of the interfaces directly beneath the region of tip contact. Hence, discrepancies were expected between the calculated and measured shape of sharp features in the $I-V$ curves. The chemical potential was taken to be 100 meV below the conduction band and the voltage drop associated with the bias voltage was assumed to take place uniformly across the stepped barrier.

Since only vertical transport was of interest, the one-dimensional Schrödinger equation for the electrons was integrated using an adaptive integration method on an original grid of 2000 points spanning the barrier region. The discontinuities at the layer interfaces were smoothed over five mesh points. As a function of bias, the transmission amplitude for electrons traveling to the right (from ground to positive bias) was calculated as a function of electron energy. The transmission probabilities were weighted with the appropriate density of states, velocity, and room temperature occupation probability for electrons traveling to the right and left. The difference between the left and right current is the net current, I, a function of the applied bias, V.

4. Results and discussion

Fig. 3 shows schematically, the effect of the voltage bias on the band structure. At zero bias, the shape of the barrier consists of two flat-topped (rectangular) steps. As the voltage bias is increased, voltage drop occurs across the GaAlAs and the InGaAs layers, thus resulting in the formation of a triangular potential well as shown in the figure. Let us now consider the transport of electrons across the heterostructure. At zero bias,

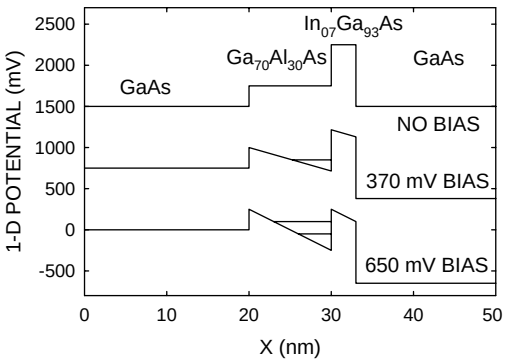

Fig. 3. Schematic showing the development of a triangular well and resonant states in the stepped-barrier heterostructure in the presence of an applied forward bias. The curves are displaced along the y-axis for clarity.

the probabilities of electrons passing through the barrier from left to right or from right to left are individually small and cancel exactly. For small biases of either sign there is some imbalance in the tunneling through the barrier resulting in a small current in the direction of the bias. For larger positive biases the triangular well formed within the barrier can support resonances.

Fig. 4 depicts the transmission probability at a bias of 350 mV and the current decomposed according to the energy of the electrons contributing to the current. Since the occupation of states declines exponentially with energy, nearly all current is associated with the lowest sharp resonance. At a bias of 570 mV the lowest resonance has moved below the conduction band, but its tail still contributes to the current. The contribution to the total current from the second resonance is almost equal to that of the tail from the first resonance. The first peak in the calculated $I-V$ curve shown in Fig. 4 results from the lowest resonance, the second peak results from the second resonance. Beyond the second peak it is debatable as to whether or not to assign the peaks to resonant states because the resonances have broadened to the point where it may be more accurate to describe them as interference effects rather than due to the formation of resonant states. At negative biases no potential well and hence no resonances develop, which results in the $I-V$ curve being almost featureless for negative voltage bias.

The measured $I-V$ curve and the calculated $I-V$ curve are qualitatively similar as shown in Fig. 5. The calculated $I-V$ curve has been scaled such that the magnitudes of the maximum current in the calculated and measured curves are equal. As predicted by the calculations, multiple NDR peaks are observed in the 0–5 V voltage range. Separations in energy of the measured features are consistent in scale with energy separations between the calculated resonant levels. Furthermore, both curves exhibit current saturation at high voltage with oscillations indicative of interference effects. As expected, the features in the calculations are sharper because of the assumed perfect coherence of the electron wave function over the width of the barrier. However, there is disagreement between the measurements and the calculations in the absolute values of the voltages at which the NDR peaks appear. In addition, the shape of the measured $I-V$ curve is different from the calculated $I-V$ curve, particularly at lower voltages. To seek out possible explanations for these discrepancies, additional calculations were carried out to account for potential deviations in the composition and thickness of the individual layers from the design values. Results of these calculations show that small changes in the assumed layer widths or potential heights do not substantially improve agreement with the experiment. Similarly, adopting gradual potential changes instead of abrupt changes does not reduce the discrepancy either. Thus, poor choice of parameters used in the simple model is not likely to be the sole source of the discrepancies between the calculated and measured $I-V$ curves.

A couple of factors have been identified as potential contributors to the observed discrepancies between the measurements and calculations. One shortcoming of the model used in this study is that the effect of the contact geometry is not accounted for in the calculations of the $I-V$ curve. Since small contact areas are involved, significant stress levels could be achieved and hence could be a factor affecting the measured $I-V$ curve. Apart from geometrical factors, chemical factors such as the composition of the

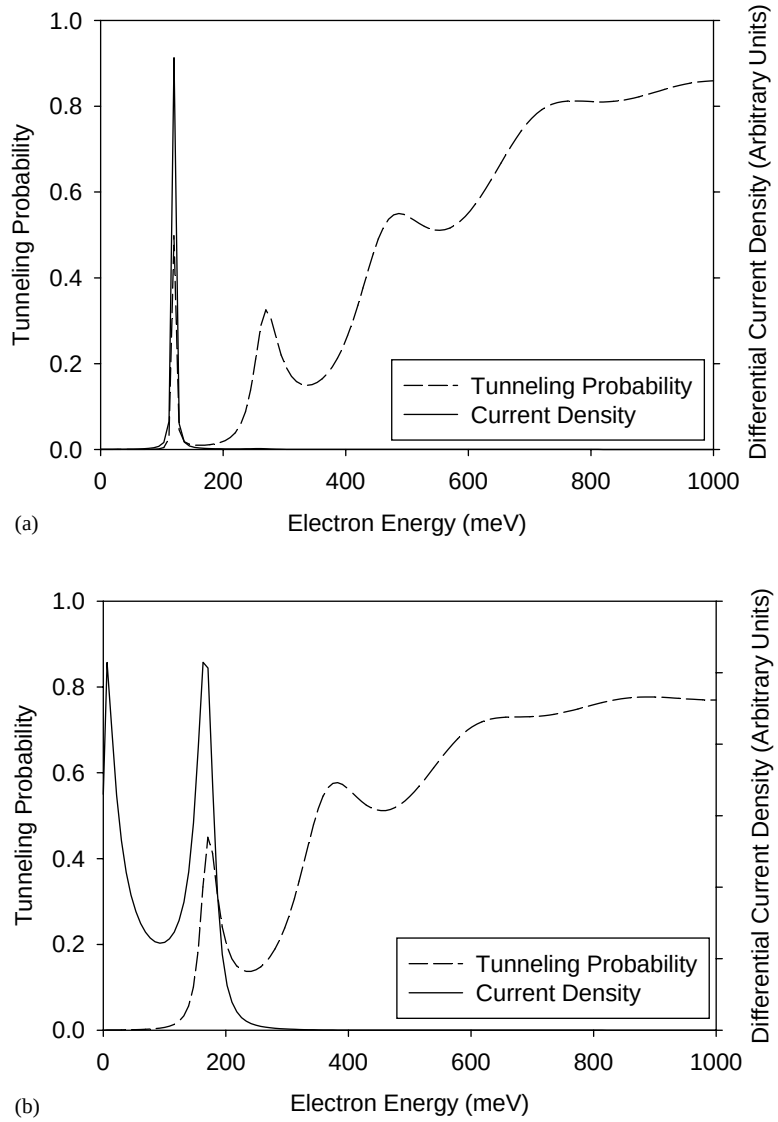

Fig. 4. Calculated transmission probability and contribution to the current as a function of electron energy for applied bias voltages of: (a) 350 mV and (b) 570 mV.

contact layer needs to be included in future calculations. In addition, achieving quantitative agreement between theory and experiment may necessitate the use of a better model for the effective potential used to calculate the effective mass that accounts for charge self-consistency as a function of current density.

5. Conclusions

Vertical electron transport has been measured through stepped GaAlAs/InAlAs/GaAs quantum barriers grown on a GaAs substrate using a setup based on a multimode AFM. $I-V$ characteristics show the presence of multiple NDR peaks.

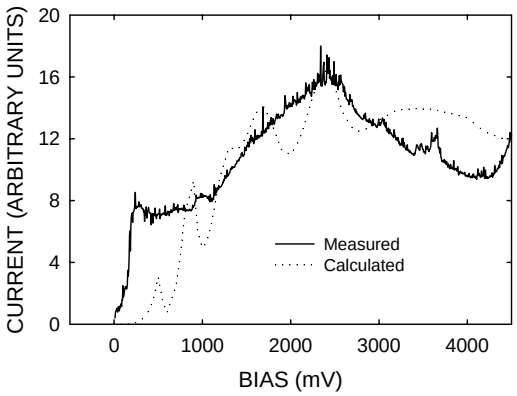

Fig. 5. Comparison between the experimentally measured and the calculated $I-V$ curves for vertical transport through the heterostructure shown in Table 1.

Numerical calculations show that the NDR peaks are related to the formation of resonant states in a potential well created by the applied voltage bias. The use of a setup based on AFM makes feasible, future work on structures with a lateral size of tens of nanometers.

Acknowledgements

The work performed by Oak Ridge National Laboratory was supported by DARPA, and the Laboratory Director's Research and Development Program of Oak Ridge National Laboratory. Oak Ridge National Laboratory is operated for the U.S. Department of Energy by Oak Ridge National Laboratory, managed by UT-Battelle, LLC, for the U.S. Department of Energy under Contract DE-AC05-00OR22725. The work performed by the University of Tennessee was supported by the NSF Grant ECS-9727208.

References

[1] A. Shik, Quantum Wells: Physics and Electronics of Two-Dimensional Systems, World Scientific, Singapore, 1997.
[2] H. Sakaki, in: G. Timp (Ed.), Nanotechnology, Springer, New York, 1999.
[3] W.K. Chen, R.H. Cheng, J. Appl. Phys. Lett. 71 (1997) 1373.
[4] Jung-Hui Tsai, Appl. Phys. Lett. 75 (1999) 2668.
[5] K.K. Likharev, Appl. Phys. Lett. 73 (1998) 2137.
[6] K. Ismail, B.S. Meyerson, P.J. Wang, Appl. Phys. Lett. 59 (1991) 973.
[7] P.A. Schulz, C.E.T. Goncalves Da Silva, Appl. Phys. Lett. 52 (1988) 960.
[8] S.J. Wang, J.C. Lin, W.R. Liou, Y.C. Luo, C.Y. Cheng, Appl. Phys. Lett. 68 (1996) 3320.
[9] Yu.N. Khanin, E.E. Vdovin, Yu.V. Dubrivskii, K.S. Novoselov, T.G. Andersson, JETP Lett. 67 (1998) 863.
[10] Yong Guo, Beng-Lin Gu, Jing-Zhi Yu, Zhong Zeng, Yoshiyuki Kawazoe, J. Appl. Phys. 84 (1998) 918.
[11] Yong Guo, Bing-Lin Gu, Zhong Zeng, Yoshiyuki Kawazoe, Phys. Lett. A 261 (1999) 114.